DOI: 10.1002/cbic.201100557

Rational Design of Fluorescent Biosensor for Cyclic di-GMP

Chun Loong Ho, Siew Lee Koh, Mary Lay Cheng Chuah, Zhen Luo, Wei Jian Tan, Donovan Kian Soon Low, and Zhao-Xun Liang*[a]

The cyclic dinucleotide c-di-GMP is now recognized as a major bacterial messenger that mediates a variety of cellular behaviors such as virulence expression and biofilm formation.[1–3] The cellular concentration of c-di-GMP is controlled by the diguanylate cyclase (DGC) activity of GGDEF domain proteins and the c-di-GMP phosphodiesterase (PDE) activity of EAL or HD-GYP domain proteins.[4] GGDEF domains catalyze the synthesis of c-di-GMP from GTP, whereas EAL and HD-GYP domains catalyze the hydrolysis of c-di-GMP to generate 5′-pGpG and GMP (Figure 1 A). Cellular c-di-GMP exerts its effect by binding to

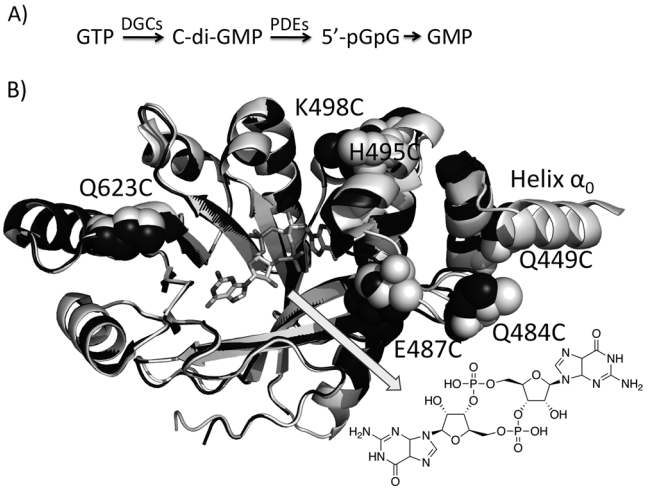

Figure 1. C-di-GMP metabolism and structure of the EAL_{FimX} domain. A) Synthesis and degradation of c-di-GMP by diguanylate cyclases (DGCs) and phosphodiesterases (PDEs). B) Structures of free (gray) and c-di-GMP-bound (black) EAL_{FimX} protein with the labeling sites highlighted. C-di-GMP is shown as sticks. Note that only the surface of the free-EAL_{FimX} is shown and that the helix α_0 for the c-di-GMP-bound structure is missing due to the unfolding of the helix.

cellular targets such as enzymes, transcriptional factors, PilZ proteins, and riboswitches.[5–12] Today, c-di-GMP signaling remains a flourishing research field with many aspects of the c-di-GMP signaling network yet to be fully unveiled.

Bacterial cells usually contain multiple copies of genes that encode c-di-GMP signaling proteins, many of which harbor catalytically incompetent GGDEF or EAL domains. Many of the GGDEF-, EAL- and HD-GYP-domain proteins also contain regulatory domains that modulate the enzymatic activity of the catalytic domains. Hence, in vitro assay of the enzymatic activities is often necessary in order to elucidate the cellular function of the proteins. Currently, in vitro assays of the enzymatic activities of GGDEF-, EAL- and HD-GYP-domain proteins require the use of radio-isotope-labeled c-di-GMP or HPLC to quantify c-di-GMP.[13–19]

It is increasingly clear that c-di-GMP plays important roles in mediating the pathogenicity of human pathogens such as *Vibrio cholerae*, *Pseudomonas aeruginosa* and *Klebsiella pneumonia*.[3,20–25] Hence, some c-di-GMP signaling proteins can be exploited for the development of antibacterial agents. The development of easy methods for screening the inhibitors of the c-di-GMP signaling proteins will facilitate lead discovery. Here we describe the design of a reagentless fluorescent biosensor for the detection of this important messenger molecule by using a natural c-di-GMP binding protein scaffold. We demonstrate that the highly sensitive biosensor can be used not only for the fast enzymatic assay of DGC and PDE activities, but also for the screening and characterization of inhibitors.

Labeling ligand-binding proteins with fluorescent dye is a knowledge-based strategy for constructing biosensors.[26–30] To design the fluorescent biosensor for c-di-GMP, a variety of c-di-GMP binding proteins were considered. The noncatalytic EAL domain of the type IV pili protein FimX[31] from *P. aeruginosa* was chosen for the following reasons. First, the EAL domain of FimX (EAL_{FimX}) binds c-di-GMP with high affinity (K_d = 120 nM),[32,33] which is ideal for the design of a biosensor with high sensitivity. Second, the free-standing EAL_{FimX} domain is a small (28 KDa) monomeric protein that exhibits great stability in solution. Third, the crystal structures of EAL_{FimX} in the c-di-GMP-free and -bound forms have been determined;[32] this allows us to take a rational design approach. Finally, binding of c-di-GMP in the EAL_{FimX} domain induces some local structural changes that can be exploited for the development of a fluorescent-dye-labeled biosensor.

Comparison of the crystal structures of EAL_{FimX} with and without c-di-GMP bound (PDB ID: 3HV8 and 3HV9) suggested that the binding of c-di-GMP does not induce large global structural changes in EAL_{FimX}.[32] Instead, it causes some local conformational changes that include side-chain rotation and structure remodeling in the N-terminal lobe region (Figure 1 B). Several surface-exposed residues (Glu487, His495, Lys498, Gln623) located near the c-di-GMP binding pocket undergo significant re-positioning or side-chain rotation. We reasoned that the position or orientation of an environmentally sensitive fluorescence dye attached to these sites could be affected by c-di-GMP binding, thus resulting in changes in the emission spectrum. Two additional residues, Gln449 and Gln484, were chosen for labeling because they are situated near the helix α_0

[a] *C. L. Ho, S. L. Koh, M. L. C. Chuah, Z. Luo, W. J. Tan, D. K. S. Low, Prof. Dr. Z.-X. Liang*
Division of Structural Biology and Biochemistry
School of Biological Sciences
Nanyang Technological University (NTU)
60 Nanyang Drive, Singapore
E-mail: zxliang@ntu.edu.sg

that undergoes unfolding upon c-di-GMP binding. Two fluorescent dyes, *N*-(2-(1-maleimidyl)ethyl)-7-(diethylamino)coumarin-3-carboxamide (MDCC) and 6-iodoacetamidofluorescein (6-IAF), were chosen because their fluorescence is sensitive to changes in the surrounding microenvironment and the thiol reactive dyes are readily available for the preparation of the protein–dye conjugate. Six mutant proteins, each containing a single cysteine residue, were prepared for dye labeling. Excluding the 449-MDCC, 498-MDCC, and 498-6IAF constructs that exhibited low labeling yield or poor stability, nine protein–dye conjugates were prepared for further assessment.

The performance of the protein–dye conjugates was evaluated by fluorescence titration. The fluorescence intensity of all the fluorophore-labeled proteins decreases upon c-di-GMP binding (Figure 2A). The ones with the most significant reduction are 484-MDCC and 484-6IAF, with decreases of 45 and 40%, respectively. For the other seven constructs, the reduction in fluorescence ranges from 3 (623-6IAF) to 30% (449-6IAF). Fitting the titration data for the best performer, 484-MDCC, to a one-site binding model yielded a dissociation constant (K_d) of 172 ± 90 nM (Figure 2B). MDCC-484 was further characterized by mass spectrometry and showed a mass of 30654.8 Da (calculated mass for the His_6-tagged protein conjugate: 30655.7 Da) with >90% dye labeling efficiency. Importantly, the presence of mono-, di-, tri-phosphate nucleotides or cyclic monophosphate nucleotides did not interfere with the performance of 484-MDCC; this indicates that the high selectivity toward c-di-GMP is not affected by the presence of the dye. Under the conditions of [c-di-GMP] < 3 μM and [biosensor] ≫ K_d, a linear relationship is maintained between fluorescence intensity and [c-di-GMP] (Figure 2C). This may be used as a standard curve; thus the biosensor provides a simple alternative to the current method of quantifying cellular c-di-GMP by liquid-chromatography mass spectrometry (LC-MS).[34]

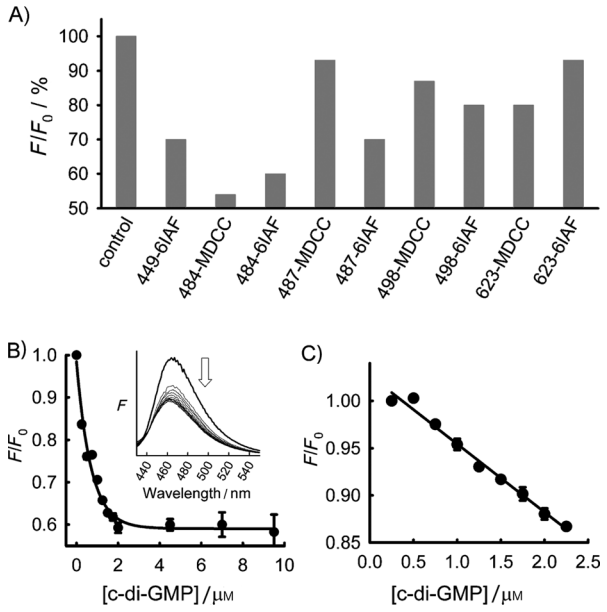

Figure 2. Fluorescence titration and binding affinity measurement. A) End point measurement of c-di-GMP-induced fluorescence changes for nine dye-conjugated biosensors. B) Fluorescence titration for 484-MDCC. Data were fit to a 1:1 binding model to yield a dissociation constant (K_d) of 172 ± 90 nM when 0.5 μM of biosensor was used. C) Linear fluorescence titration curve obtained under the conditions of [c-di-GMP] < 3 μM and [biosensor] (10 μM) ≫ K_d. Titration conditions: 10 mM mPBS, 137 mM NaCl, 2.7 mM KCl, pH 7.0, 23 °C.

We tested whether the best-performing MDCC-484 can be used to assay the enzymatic activities of DGC and PDE proteins. To be practically useful for enzymatic assay, the biosensor must be stable over the course of the enzymatic assay and able to respond to the formation of enzymatic product or depletion of substrate in a near real-time fashion. 484-MDCC is rather stable under the experimental conditions, as evidenced by the negligible change in fluorescence signal after long incubation (>2 h). Using the PDE protein RocR (*P. aeruginosa*) and the DGC protein DGC2 (*A. xylinum*) as model systems,[15–17] we found that 484-MDCC is capable of reporting the synthesis of c-di-GMP by DGC2 and the degradation of c-di-GMP by RocR in real time. As shown in Figure 3A and C, the decrease in fluorescence in the DGC2 assay indicates the accumulation of c-di-GMP; whereas the observed increase in fluorescence for RocR indicates the depletion of c-di-GMP. Importantly, fluorescence intensity increases or decreases almost instantly upon the addition of GTP or c-di-GMP. The dependence of the rate on substrate concentration also indicates that the biosensor is capable of reporting the dose-dependent change of enzymatic activities. The linear relationship between concentration and fluorescence intensity illustrated in Figure 2C allows the calculation of initial velocities (V_0, μM min^{-1}) from the slopes of the curves in Figure 3A and C. Parallel HPLC enzymatic assays yielded similar V_0 values; this indicates that the binding of c-di-

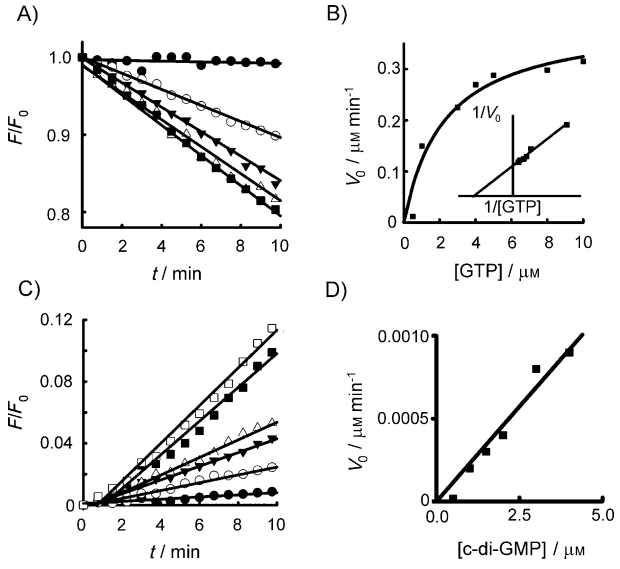

Figure 3. Assay of DGC and PDE enzymatic activities using the 484-MDCC biosensor. A) Substrate concentration-dependence of the DGC activity of DGC2; ●: 0.5, ○: 1.0, ▼: 3.0, △: 5.0, ■: 10.0 μM. B) Michaelis–Menten plot for DGC2. Inset: Lineweaver–Burk plot. C) Substrate concentration dependence of the PDE activity of RocR; □: 4.0; ■: 3.0, △: 2.0, ▼: 1.5, ○: 1.0, ●: 0.5 μM. D) Steady-state kinetics measurements for RocR. Reaction conditions: 100 mM Tris·HCl, 50 mM KCl, pH 8.0, 23 °C.

GMP to biosensor is not rate-limiting. The initial velocities were plotted against substrate concentrations to obtain steady-state kinetic parameters (Figure 3B, D). V_{max} (0.4 μM min^{-1}) and K_M (2.3 μM) were readily obtained for DGC2. Note that the values are different from those reported for DGC2 previously,[16] largely because the protein used in the current study was significantly stabilized by the use of detergent in protein preparation (Koh et al., unpublished results). As for RocR, only the second-order rate constant or specificity constant k_{cat}/K_M (or V_{max}/K_M) could be obtained because K_M (3.2 μM)[17] is close to the upper limit of [c-di-GMP] (3 μM) that can be detected by the biosensor in the linear range. If k_{cat} and K_M need to be measured, the 3 μM upper limit can be raised by weakening the binding through mutagenesis. The continuous-assay method with the biosensor is much faster than the traditional enzymatic-assay methods for PDE and DGC proteins, and does not require the preparation and use of radio-isotope-labeled substrate.

C-di-GMP is known to mediate pathogenicity and biofilm formation in many pathogenic bacteria.[3,21,22] DGCs and PDEs are currently being considered as potential targets for developing antimicrobial drugs to suppress virulence expression or control biofilm formation. A facile method of screening for inhibitors of DGC and PDE proteins would be advantageous. By using a fluorescence multi-plate reader, we demonstrate that the 484-MDCC biosensor can be used for the fast screening of enzyme inhibitors. For example, in an end-point measurement experiment with a collection of nucleotides, the GTP analogue guanosine-5′-*O*-(1-thiotriphosphate) (Rp-GTP-α-S) was quickly identified along with GDP as having a significant inhibitory effect on DGC2 (Figure 4A). The inhibitory effect was validated by measuring the enzymatic efficiency by the traditional HPLC method (data not shown). Curiously, we observed an enhanced fluorescence decrease for CTP and TTP. Because no interference was observed for CTP and TTP in the titration experiment, such a phenomenon is likely due to the interaction of the nucleotides with DGC2 rather than with the biosensor. We speculate that the two nucleotides might interact with the flavin-binding PAS domain of DGC2 and modulate the activity of the GGDEF domain. In another experiment, we showed that 484-MDCC can be used for the characterization of inhibitors by using it to measure the IC_{50} of Ca^{2+} for RocR. This ion is known to be an effective inhibitor of the EAL-domain-containing PDEs, presumably by replacing the catalytic Mg^{2+} ion.[13,17] The initial velocities of RocR at various $CaCl_2$ concentrations were measured. The data were fit to a sigmoidal dose–response model to give the IC_{50} (141 ± 10 μM; Figure 4B). Together, the two experiments demonstrate that the 484-MDCC sensor is a useful tool for the screening and characterization of enzyme inhibitors.

Considering that Cys484 is not located in the c-di-GMP binding pocket, the observed fluorescence change upon the binding of c-di-GMP cannot be attributed to the exclusion of MDCC from the c-di-GMP binding pocket. Hence, it is not immediately apparent how the binding of c-di-GMP causes a decrease in the fluorescence intensity of the dye tethered to Cys484. We performed modeling studies with the knowledge-based Rosetta Design package,[35,36] which employs a Metropolis–Monte Carlo search method to explore the possible binding mode of MDCC on the surface of c-di-GMP-free EAL_{FimX} (PDB ID: 3HV9). Instead of treating the MDCC-modifying Cys484 as a noncanonical amino acid that requires the creation of a rotamer library for conformation sampling,[37] we generated a conformer library of MDCC and imposed a distance constraint on the electrophilic carbon atom of MDCC and sulfur atom of Cys484 to mimic the covalent linkage. With the randomly generated starting protein–MDCC structures all having MDCC placed close to protein surface, simultaneous sampling of the side-chain conformations and MDCC position generated models (decoys) that were ranked by the total score and protein–MDCC interaction energy. The lowest interaction energy was found when MDCC was tucked under the terminal helix α_0 (Figure 5A). According to the model, interactions between MDCC and several nonpolar residues are likely to contribute to the stabilization of this low-energy conformation (Figure 5B).

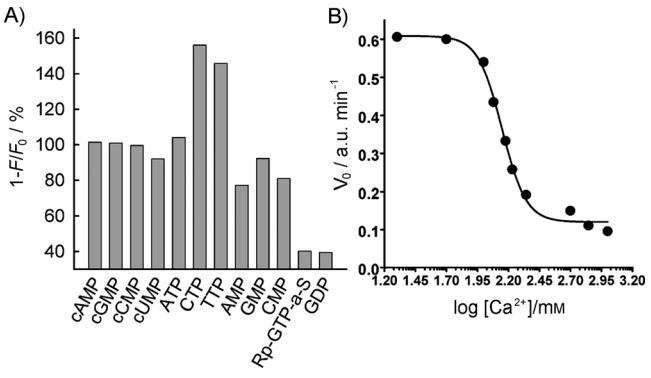

Figure 4. Inhibition measurement with the 484-MDCC biosensor. A) Screening of the inhibitors for the DGC protein DGC2 by using a Tecan Infinite 200 PRO fluorescence multi-plate reader and 96-well plates. Experimental conditions: reaction time = 10 min, 100 mM Tris·HCl, 50 mM KCl, pH 8.0, 23 °C. B) Measurement of the IC_{50} value of the inhibitor Ca^{2+} for RocR. The data were fit to a one-site inhibition model to yield the IC_{50} value. Experimental conditions: 100 mM Tris·HCl, 50 mM KCl, pH 8.0, 23 °C.

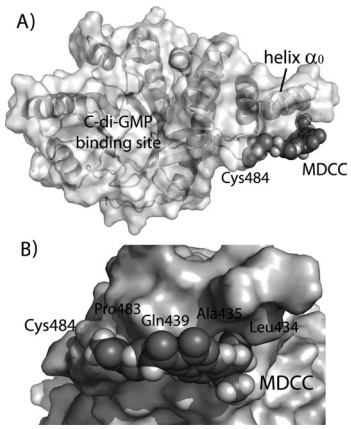

Figure 5. Model of the 484-MDCC sensor in the c-di-GMP-free state. A) The lowest-energy model with the MDCC dye tucked under helix α_0. B) Interaction between MDCC and the residues of helix α_0. The stabilization and protection from helix α_0 would be lost when the binding of c-di-GMP triggers the unfolding of the helix.

In the light of the crystallographic observation that helix α_0 unfolds upon c-di-GMP binding (Figure 1B),[32] the modeling results would suggest that the reduction in fluorescence intensity upon c-di-GMP binding is caused by the "melting" of helix α_0 and is accompanied by an increase in polarity in the surrounding microenvironment for MDCC.

In summary, we have described here the design of a protein-based c-di-GMP fluorescent biosensor that takes advantage of the local structural changes in a c-di-GMP-binding EAL domain scaffold. Covalent modification of the protein with a fluorophore at various sites led to the identification of a protein–dye conjugate (484-MDCC) that responds to c-di-GMP with high sensitivity (sub-μM K_d) and high selectivity in real-time. We have demonstrated that the biosensor can be used not only for the facile assay of the enzyme activities for c-di-GMP signaling proteins, but also for the measurement of IC_{50} and high-throughput screening of enzyme inhibitors. We expect the biosensor to be a valuable tool for the study of c-di-GMP signaling proteins and the development of inhibitors targeting c-di-GMP signaling pathways.

Experimental Section

Cloning, expression and purification of the EAL_{fimx} protein: The DNA encoding EAL_{FimX} ($FimX_{431-691}$) was amplified from the full-length *fimX* gene by PCR and cloned into pET-28b vector (Novagen). Prior to the mutation of the labeling sites, the intrinsic cysteine residues at positions 590 and 599 were mutated to serine by using KAPA HiFi DNA polymerase. The plasmid was used as the template for mutagenesis to introduce the six cysteine sites for labeling: Q449C, Q484C, E487C, H495C, K498C and Q623C. The plasmids were transformed into *Escherichia coli* BL21(DE3) by using heat shock. For protein expression, the transformed *E. coli* was grown in lysogeny broth (LB; 2 mL) supplemented with kanamycin (50 mg L^{-1}) and grown overnight at 37 °C with shaking at 200 rpm. The seed culture was then used to inoculate culture (0.8 L) with kanamycin (50 mg L^{-1}) and grown at 37 °C and 200 rpm to reach an OD_{600} nm of 0.8. The culture was induced with IPTG (0.5 mM) and incubated at 16 °C and 160 rpm for 20 h. The cells were then spun down at 11300 *g* for 8 min. The cell pellet was collected and suspended in lysis buffer (10 mL, 50 mM Na_2HPO_4, 300 mM NaCl, 10% glycerol, 1 mM dithiothreitol (DTT)). The cell suspension was lysed by sonication, spun down at 48400 rpm for 30 min. The supernatant was then filtered through a 0.45 μm cellulose filter. The filtrate was incubated with buffer (1 mL) containing nickel-nitrilotriacetic acid (Ni-NTA) resin for 1 h at 4 °C. Resins were packed onto a small column and washed with lysis buffer supplemented with a gradient of imidazole (0–50 mM) and finally eluted with imidazole (300 mM). The fractions that contained the recombinant protein were treated with the c-di-GMP phosphodiesterase RocR (along with 10 mM $MgCl_2$ and 10 mM DTT) to remove the trace amount of c-di-GMP bound by the protein. The protein mixture was incubated on ice for three hours before the protein was purified by gel-exclusion chromatography on an ÄKTA FPLC system equipped with a Superdex 200 HR 16/60 column (GE Healthcare). The protein was concentrated for storage and fluorescent dye labeling.

Cloning, expression and purification of DGC and PDE proteins: The expression and purification of the c-di-GMP phosphodiesterase RocR has been described previously.[15,17] The DGC2 gene was inserted into pET-28b(+) between the NdeI and XhoI sites.[16] The plasmid was transformed into *E. coli* BL21 (DE3) by heat shock. The cells were grown in LB with kanamycin (30 mg L^{-1}) at 37 °C, overnight. 1% of the overnight culture was then inoculated into LB (800 mL), and the cells were grown at 37 °C with vigorous shaking (200 rpm) until the OD_{600} reached 0.6. The supplement riboflavin (1 μg L^{-1}) was added to the culture before IPTG induction (0.5 mM), and the culture was grown at 16 °C for 16–18 h. The cells were harvested by centrifugation at 11300 *g* for 15 min. All the subsequent purification steps were performed at 4 °C. The cell pellet was resuspended in lysis buffer (50 mM phosphate, 200 mM NaCl, 5 mM β-mercaptoethanol, 5% glycerol, 1% Triton X-100, 0.2 mM phenylmethanesulfonylfluoride, 20 mM imidazole, pH 7.0) and lysed by sonication. After the solution had been centrifuged at 48400 *g* for 30 min, the supernatant was filtered and then loaded onto prepacked Ni-NTA resin. The resin was washed with a gradient of imidazole (0–50 mM) and eluted with imidazole (600 mM). The protein was desalted and exchanged into the final buffer (50 mM Tris·HCl, 50 mM NaCl, 10% glycerol, 1 mM DTT, pH 8.0) either on a PD-10 or a Superdex-200 column (both GE Healthcare). The resulting yellow protein was concentrated in an Amicon concentrator (Millipore), aliquoted and stored at −80 °C.

Protein modification by thiol reactive fluorophores: The purified protein was exchanged into the modified phosphate-buffered saline solution (mPBS; 137 mM NaCl, 2.7 mM KCl, 5.37 mM Na_2HPO_4, 1.76 mM KH_2PO_4, pH 7.0, degassed with N_2 for 30 min). The protein solution was treated with tris-(2-carboxyethyl)phosphine (TCEP, 50 mM) for 30 min on ice to ensure that the thiols were reduced. The protein solution was buffer exchanged twice with mPBS containing TCEP (2 mM) and moved into an anaerobic chamber. The fluorescent dye was dissolved in DMSO to prepare a 10 mM solution. The solution was then further diluted to 2 mM with mPBS containing TCEP (2 mM). This dye solution was then added to the protein solution at a dye/protein ratio of 5:1. The reaction mixture was gently shaken at 4 °C overnight. The labeled protein was dialyzed by using Snakeskin dialysis tubing with 10000 MWCO against mPBS containing 5% glycerol and DTT (1 mM). Labeled protein was dialyzed overnight and concentrated to approximately 0.5 mM before being aliquoted and flash frozen for storage at −80 °C.

Fluorescence titration: Dissociation constants (K_d) were determined by titrating the biosensors with enzymatically synthesized c-di-GMP.[38,39] The protein was titrated with c-di-GMP (0 to 10 μM) by using a fluorescence spectrometer (Cary Eclipse, Varian) and a semi-micro cuvette. Proteins labeled with MDCC was excited at 419 nm, and emissions were recorded from 430 to 600 nm. Proteins labeled with 6-IAF were excited at 491 nm, and emissions were recorded from 500 to 700 nm. The emission maxima at 466 (for MDCC) and 516 nm (for 6-IAF) were recorded for K_d determination. Titrations were carried out in mPBS (10 mM; 137 mM NaCl, 2.7 mM KCl, pH 7.0, 23 °C). The mono-, di-, tri- or cyclic monophosphate nucleotides (10 μM) were used to assay the selectivity.

Enzymatic assays (PDE and DGC): Enzymatic assays of DGC and PDE were performed with GTP and c-di-GMP as substrate, respectively. A Tecan Infinite 200 PRO multi-plate reader equipped with a fluorescence detector was used. The reaction kinetics was observed with the I-Control software, with measurements set to an excitation wavelength of 419 nm and emissions recorded at 466 nm. For the PDE activity assay, c-di-GMP, Mg^{2+} (10 mM), and 484-MDCC biosensor ($\leq$10 μM) were first equilibrated in the reaction buffer (100 mM Tris·HCl, 50 mM KCl, pH 8.0). RocR was added to start the enzymatic reaction, and the fluorescence intensity was recorded continuously. For the DGC activity assay, DGC2 (1 μM),

Mg^{2+} (10 mM) and the 484-MDCC biosensor (10 μM) were equilibrated in the buffer solution described above. Substrate GTP was added to start the reaction, and the fluorescent intensity was recorded continuously.

Inhibitor screening for DGC proteins: Inhibitors were screened by using a TECAN Infinite 200 PRO multi-plate reader equipped with a fluorescence detector. The reaction mixture was prepared in the reaction buffer (100 mM Tris-HCl, 50 mM KCl, pH 8.0) in a black 96-well plate with a clear flat bottom. DGC2 (0.5 μM), 484-MDCC biosensor (10 μM), Mg^{2+} (10 mM) and inhibitor (100 μM) were equilibrated briefly at room temperature before the reaction was started by the addition GTP (100 μM). The fluorescence intensities for all the wells containing reaction mixture were recorded continuously.

IC_{50} measurement: IC_{50} values were measured by using the 484-MDCC biosensor to monitor the initial velocities of RocR at various Ca^{2+} concentrations (0, 20, 50, 100, 120, 150, 170, 200, 220, 500, 700, and 1000 μM). The reaction mixture was prepared in the reaction buffer (100 mM Tris·HCl, 50 mM KCl, pH 8.0) in a fluorescence quartz cuvette. The 484-MDCC biosensor (10 μM) was briefly incubated with Mg^{2+}, c-di-GMP, and $CaCl_2$ before the addition of RocR. Measurements were taken on the fluorescence spectrometer with the same excitation and emission wavelengths described above. The initial velocities were obtained as the slopes of the linear portion of time-dependent plots. The data were fit to a 1:1 inhibition model to yield the IC_{50} value in Prism (Graphpad).

Liquid chromatograph (LC)-coupled mass spectrometry: The mass of MDCC-484 was measured on a high-resolution LTQ orbitrap spectrometer (Thermo Scientific).

Modeling of the protein–MDCC conjugate: The modeling was performed by using the RosettaDesign 3.2 package.[35,36] After the PDB file (PDB ID: 3HV8) had been cleaned, the side chains of the starting model were repacked by using the Rosetta fixed-backbone protocol. The model of the MDCC dye was built in Maestro (Schrödinger) with energy minimization. A conformer library for MDCC was generated by using the ConfGen program.[40] The parameter files required by Rosetta were generated from the PDB and MOL files by using the command molfile_to_params. Starting structures were generated by manually placing the MDCC conformers near the Cyc484 residue in random orientations, with a distance of 1.8 ± 0.2 Å; between the sulfur atom of Cyc484 and the nucleophilic carbon of MDCC. A constraint (cst) file was created to specify the distance (1.8 ± 0.2 Å) between the sulfur atom of Cys484 and the nucleophilic carbon of MDCC. With input files that combined the protein and the MDCC conformers, the enzyme_design protocol was used to repack the side chains (packing options: -ex1, -ex2, -use_input_sc, -linmem_ig10, -soft_rep_design).[41] The generated decoys were ranked based on the total score and protein–dye interaction energy.

Acknowledgements

This work was supported by an AcRF grant from the Ministry of Education, Singapore (to Z.-X.L.). We thank Dr. Kai Tang and Xueming Dong for their assistance with the mass spectrometry measurements.

Keywords: biofilms · biosensors · diguanylate cyclases · nucleotides · phosphodiesterases

[1] U. Römling, M. Gomelsky, M. Y. Galperin, *Mol. Microbiol.* **2005**, *57*, 629–639.
[2] R. Hengge, *Nat. Rev. Microbiol.* **2009**, *7*, 263–273.
[3] P. A. Cotter, S. Stibitz, *Curr. Opin. Microbiol.* **2007**, *10*, 17–23.
[4] U. Jenal, J. Malone, *Annu. Rev. Genet.* **2006**, *40*, 385–407.
[5] P. Ross, R. Mayer, H. Weinhouse, D. Amikam, Y. Huggirat, M. Benziman, E. de Vroom, A. Fidder, P. de Paus, L. A. Sliedregt, *J. Biol. Chem.* **1990**, *265*, 18933–18943.
[6] W. Haim, S. Shai, A. Dorit, S. Yehudit, V. Gail, O. Patricia, B. Moshe, *FEBS Lett.* **1997**, *416*, 207–211.
[7] D. Amikam, M. Y. Galperin, *Bioinformatics* **2006**, *22*, 3–6.
[8] J. W. Hickman, C. S. Harwood, *Mol. Microbiol.* **2008**, *69*, 376–389.
[9] D. A. Ryjenkov, R. Simm, U. Romling, M. Gomelsky, *J. Biol. Chem.* **2006**, *281*, 30310–30314.
[10] N. Sudarsan, E. R. Lee, Z. Weinberg, R. H. Moy, J. N. Kim, K. H. Link, R. R. Breaker, *Science* **2008**, *321*, 411–413.
[11] J. T. Pratt, R. Tamayo, A. D. Tischler, A. Camilli, *J. Biol. Chem.* **2007**, *282*, 12860–12870.
[12] P. D. Newell, R. D. Monds, G. A. O'Toole, *Proc. Natl. Acad. Sci. USA* **2009**, *106*, 3461–3466.
[13] A. J. Schmidt, D. A. Ryjenkov, M. Gomelsky, *J. Bacteriol.* **2005**, *187*, 4774–4781.
[14] D. A. Ryjenkov, M. Tarutina, O. V. Moskvin, M. Gomelsky, *J. Bacteriol.* **2005**, *187*, 1792–1798.
[15] F. Rao, Y. Qi, H. S. Chong, M. Kotada, B. Li, J. Lescar, K. Tang, Z.-X. Liang, *J. Bacteriol.* **2009**, *191*, 4722–4731.
[16] Y. Qi, F. Rao, Z.-X. Liang, *Biochemistry* **2009**, *48*, 10275–10285.
[17] F. Rao, Y. Yang, Y. Qi, Z. X. Liang, *J. Bacteriol.* **2008**, *190*, 3622–3631.
[18] M. Christen, B. Christen, M. Folcher, A. Schauerte, U. Jenal, *J. Biol. Chem.* **2005**, *280*, 30829–30837.
[19] F. Rao, R. Y. See, D. Zhang, D. C. Toh, Q. Ji, Z.-X. Liang, *J. Biol. Chem.* **2010**, *285*, 473–482.
[20] A. D. Tischler, A. Camilli, *Infect. Immun.* **2005**, *73*, 5873–5882.
[21] M. He, Z. M. Ouyang, B. Troxell, H. J. Xu, A. Moh, J. Piesman, M. V. Norgard, M. Gomelsky, X. F. Yang, *PLoS Pathog.* **2011**, *7*, e1002133.
[22] J. G. Malone, T. Jaeger, C. Spangler, D. Ritz, A. Spang, C. Arrieumerlou, V. Kaever, R. Landmann, U. Jenal, *PLoS Pathog.* **2010**, *6*, e1000804.
[23] J. M. Dow, Y. Fouhy, J. F. Lucey, R. P. Ryan, *Mol. Plant-Microbe Interact.* **2006**, *19*, 1378–1384.
[24] B. Lim, S. Beyhan, F. H. Yildiz, *J. Bacteriol.* **2007**, *189*, 717–729.
[25] J. J. Wilksch, J. Yang, A. Clements, J. L. Gabbe, K. R. Short, H. Cao, R. Cavaliere, C. E. James, C. B. Whitchurch, M. A. Schembri, M. L. C. Chuah, Z.-X. Liang, O. L. Wijburg, A. W. Jenney, T. Lithgow, R. A. Strugnell, *PLoS Pathog.* **2011**, *7*, e1002204.
[26] H. X. Wang, E. Nakata, I. Hamachi, *ChemBioChem* **2009**, *10*, 2560–2577.
[27] R. Sakaguchi, K. Tainaka, N. Shimada, S. Nakano, M. Inoue, S. Kiyonaka, Y. Mori, T. Morii, *Angew. Chem.* **2010**, *122*, 2196–2199; *Angew. Chem. Int. Ed.* **2010**, *49*, 2150–2153.
[28] S. Kunzelmann, M. R. Webb, *J. Biol. Chem.* **2009**, *284*, 33130–33138.
[29] M. P. Okoh, J. L. Hunter, J. E. T. Corrie, M. R. Webb, *Biochemistry* **2006**, *45*, 14764–14771.
[30] S. Tsukiji, H. X. Wang, M. Miyagawa, T. Tamura, Y. Takaoka, I. Hamachi, *J. Am. Chem. Soc.* **2009**, *131*, 9046–9054.
[31] B. Huang, C. B. Whitchurch, J. S. Mattick, *J. Bacteriol.* **2003**, *185*, 7068–7076.
[32] M. V. A. S. Navarro, D. N. N. Bae, Q. Wang, H. Sondermann, *Structure* **2009**, *17*, 1104–1116.
[33] Y. Qi, M. L. C. Chuah, X. Dong, K. Xie, Z. Luo, K. Tang, Z.-X. Liang, *J. Biol. Chem.* **2011**, *286*, 2910–2917.
[34] R. Simm, M. Morr, U. Remminghorst, M. Andersson, U. Römling, *Anal. Biochem.* **2009**, *386*, 53–58.
[35] R. Das, D. Baker, *Annu. Rev. Biochem.* **2008**, *77*, 363–382.
[36] A. Leaver-Fay, M. Tyka, S. M. Lewis, O. F. Lange, J. Thompson, R. Jacak, K. W. Kaufman, P. D. Renfrew, C. A. Smith, W. Sheffler, I. W. Davis, S. Cooper, A. Treuille, D. J. Mandell, F. Richter, Y.-E. A. Ban, S. J. Fleishman, J. E. Corn, D. E. Kim, S. Lyskov, M. Berrondo, S. Mentzer, Z. Popovic, J. J. Havranek, J. Karanicolas, R. Das, J. Meiler, T. Kortemme, J. J. Gray, B. Kuhlman, D. Baker, P. Bradley, *Methods Enzymol.* **2010**, *487*, 545–574.
[37] A. Gulyani, E. Vitriol, R. Allen, J. R. Wu, D. Gremyachinskiy, S. Lewis, B. Dewar, L. M. Graves, B. K. Kay, B. Kuhlman, T. Elston, K. M. Hahn, *Nat. Chem. Biol.* **2011**, *7*, 437–444.

[38] F. Rao, S. Pasunooti, Y. Ng, W. Zhuo, L. Lim, W. Liu, Z.-X. Liang, *Anal. Biochem.* **2009**, *389*, 138 – 142.
[39] S. Pasunooti, W. Surya, S. N. Tan, Z. X. Liang, *J. Mol. Catal. B* **2010**, *67*, 98 – 103.
[40] K. S. Watts, P. Dalal, R. B. Murphy, W. Sherman, R. A. Friesner, J. C. Shelley, *J. Chem. Inf. Model.* **2010**, *50*, 534 – 546.
[41] F. Richter, A. Leaver-Fay, S. D. Khare, S. Bjelic, D. Baker, *PLoS One* **2011**, *6*, e19230.

Received: August 31, 2011
Published online on October 21, 2011

